

1

2 **Supplemental Table 1: Baseline characteristics of long RNA sequencing cohort**

Measures	Overall (18)	Cr Low (9)	Cr High (9)	p-value
Age at admission, Years	69 (64-75)	68 (68-72)	74 (70-77)	0.04
Male Sex, %	28 (5/18)	33 (3/9)	22 (2/9)	0.5
Creatinine (mg/dL)	1(0.8-1.3)	0.8(0.7-0.9)	1.22(1.1-1.6)	<b>&lt;0.01</b>
Diabetes, %	22 (4/18)	44 (4/9)	0 (0/9)	0.01
EGFR, ml/min/1.73m2	69(51-89)	85(70-94)	49(28-58)	<0.01

***Median (1st,3d quartile)***

*\*Fisher's exact test*

3

4

5

6

7

8

9

10

11

12

13

14

15

16

17

18

19

20

**Supplemental Table 2: Primers list**

Sl.No.	Gene Names	Sequences (5 → 3)
1.	<i>LCN2</i> F	CCA CCT CAG ACC TGA TCC CA
	<i>LCN2</i> R	CCC CTG GAA TTG GTT GTC CTG
2.	<i>IL18</i> F	TCT TCA TTG ACC AAG GAA ATC CG
	<i>IL18</i> R	TCC GGG GTG CAT TAT CTC TAC
3.	<i>HAVCR1</i> F	TGGCACTGTGACATCCTCAGA
	<i>HAVCR1</i> R	GCAACGGACATGCCAACATA
4.	<i>TIMP3</i> F	TTT GCC CTT CTC CTC CAA TAC
	<i>TIMP3</i> R	TCT GCT TGT TGC CTT TGA
5.	<i>FST</i> F	GCC TAT GAG GGA AAG TGT ATC AA
	<i>FST</i> R	CCC AAC CTT GAA ATC CCA TAA AC
6.	<i>BMP6</i> F	GCT CTC CAG TGC TTC AGA TTA C
	<i>BMP6</i> R	CAC ATA CAG CTA ATG CTT CCT
7.	<i>SMAD7</i> F	GAA ATC CAA GCA CCA CCA AAC
	<i>SMAD7</i> R	CAC ACT CAC ACT CAC ACA CA
8.	<i>EGFR</i> F	AGT AAC AAG CTC ACG GAG TT
	<i>EGFR</i> R	CAA GGA CCA CCT CAC AGT TAT TT
9.	<i>CST3</i> F	CCTCCATGACCAGCCACATCT
	<i>CST3</i> R	AGG CGT CCT GAC AGG TGG ATT T
10.	<i>GAPDH</i> F	GGA GCG AGA TCC CAA AAT
	<i>GAPDH</i> R	GGC TGT TGT CAT ACT TCT CAT GG

**Supplemental Table 3: DIANA mirPath v.3 KEGG comparative pathway****analysis**

	p-value	#genes	#miRNAs
Prion diseases	1.26E-13	9	4
Lysine degradation	9.41E-07	18	4
Proteoglycans in cancer	1.52E-06	61	6
AMPK signaling pathway	2.37E-06	49	5
Chronic myeloid leukemia	1.46E-05	29	6
Cell cycle	4.08E-05	45	6
TGF beta signaling pathway	5.82E-05	27	6
Signaling pathways regulating pluripotency of stem cells	8.06E-05	46	5
Other types of O-glycan biosynthesis	0.000242	11	4

*P-value threshold: 0.001*

*FDR correction*

22

23

24

25

26

27

28

29

**Supplemental Table 4:****KEGG pathways for GSE30718 dataset**

Measures	Overall (18)	HFpEF (12)	Controls (6)
Complement and coagulation cascades	4.280836032	6.29E-07	2.05E-04
Pathogenic Escherichia coli infection	4.611627907	7.22E-06	0.001177138
Pathways in cancer	1.895842579	1.21E-05	0.001320098
Mineral absorption	4.558880529	1.96E-05	0.001419735
Regulation of actin cytoskeleton	2.480824872	2.18E-05	0.001419735
Adherens junction	3.816335594	2.66E-05	0.001447672
Phagosome	2.503021726	2.79E-04	0.011653853
PI3K-Akt signaling pathway	1.91065563	2.86E-04	0.011653853
Focal adhesion	2.230498422	4.42E-04	0.016027348
Bacterial invasion of epithelial cells	3.141931175	6.49E-04	0.021144503
Leukocyte transendothelial migration	2.642078488	7.65E-04	0.022659831
Proteoglycans in cancer	2.13501292	0.001049365	0.028507757
Parathyroid hormone synthesis, secretion and action	2.592227951	0.001398017	0.035057975

31

32 **Supplemental Table 5: eQTL analysis**

33

---

IVW

---

Gene Symbol	Phenotype	SNPs	Estimate (95% CI)	P-value	Heterogeneity p-value
FST	eGFR	3	0.005 (0.002 – 0.007)	5.5E-5	0.45
SMAD7	eGFR	3	-0.002 (-0.004 – 0.0005)	0.01	0.75

---

34 A Bonferroni-corrected association  $p < (0.05/5 \text{ genes}=0.01)$  was considered significant.

35

36

37

38

39

40

41

42

43

44

45

46

47

48

49

50

51

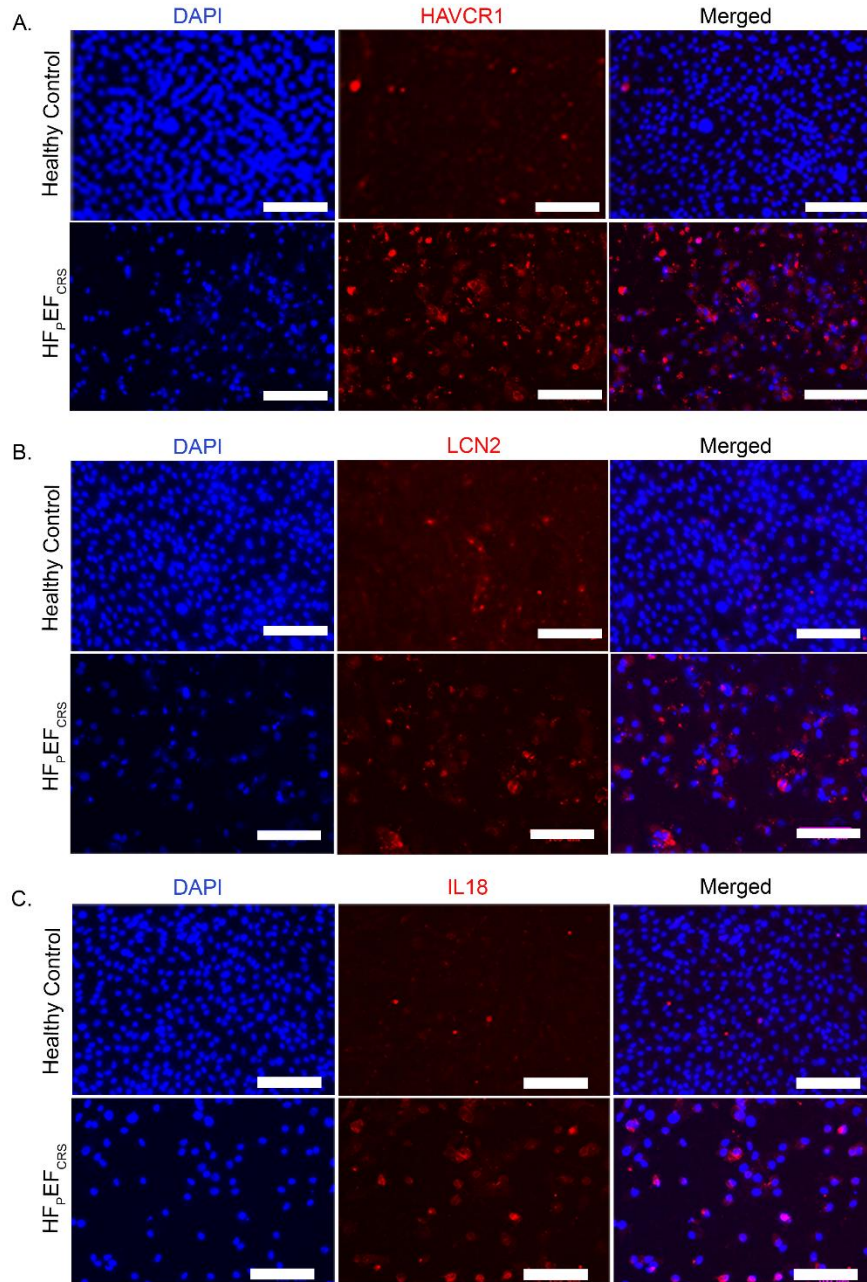
52

**Supplemental Table 6: Antibodies used**

Antibody Names	Company	Catalogue No
CD81 (clone:5A6)	Biolegend (San Diego, CA, USA)	349514
CD63 (clone: polyclonal)	Abcam (Cambridge, UK)	ab216130
Alix (clone: polyclonal)	Abcam	ab88388
Syntenin (clone: EPR8102)	Abcam	ab133267
58K Golgi protein (clone: 58K-9)	Abcam	ab27043
IL18 (clone: polyclonal)	Thermo Fisher Scientific (Waltham, MA, USA)	PA5-110679
LCN2 (clone ERP5084)	Abcam	ab125075
HAVCR1 (KIM1) (clone: polyclonal)	Thermo Fisher Scientific	PA5-79345
Goat anti-Rabbit IgG (clone: polyclonal)	Thermo Fisher Scientific	A-21428
Alexa Fluor 555 (clone: polyclonal)	Thermo Fisher Scientific	A-31572
Anti-Mouse IgG (clone: polyclonal)	Agilent (Santa Clara, CA, USA)	P0447
Anti-Rabbit IgG (clone: polyclonal)	Cell Signaling Technology (Danver, MA, USA)	7074S

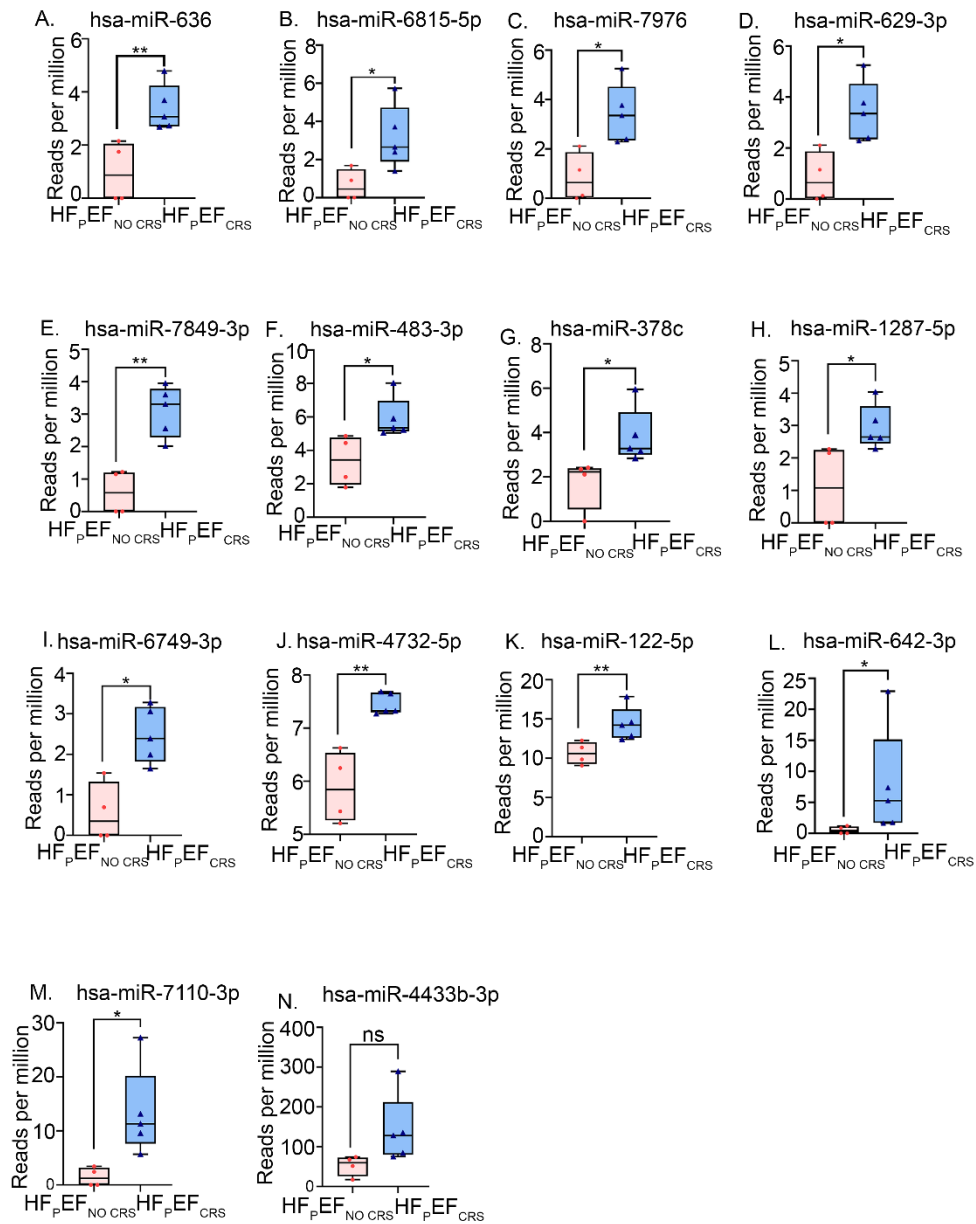
**Supplemental Table 7: Cells used for KOC and proximal tubule epithelial cell cultures**

Cell Names	Company	Catalogue No	Source
hRPTEC -Primary Human Renal Proximal Tubule Epithelial Cells	Lonza (Basel, Switzerland)	CC-2553	Normal human donor tissue
hMVEC -Primary Human Glomerular Microvascular Endothelial Cells	Cell Systems (Kirkland, WA, USA)	ACBRI 128	Normal human donor tissue



56

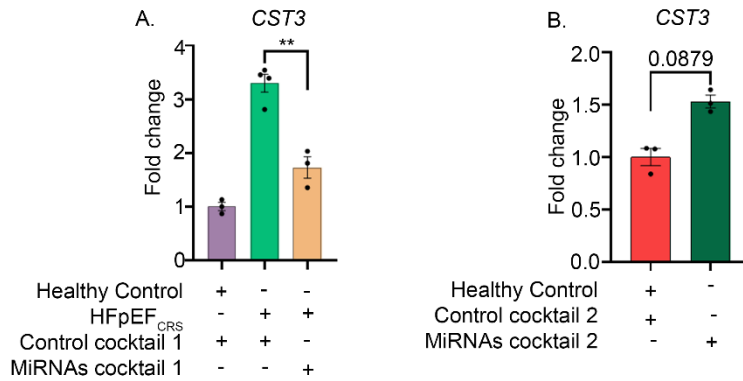
57 **Supplemental Figure 1: Immunofluorescence study of kidney injury markers:** Immunofluorescence  
 58 study showing increased expression of HAVCR1, LCN2 and IL18 in the epithelial cells of HF<sub>p</sub>EF<sub>CRS</sub>  
 group compared to Healthy Control group (Magnification= 100 $\mu$ m). Representative images of three independent  
 experiments conducted.



61

62 **Supplemental Figure 2: (A-N)** Box and whisker plots showing significant higher expression (reads per  
63 million) of different miRNAs in the EVs of the HFpEF<sub>CRS</sub> group compared to the HFpEF<sub>NO CRS</sub>. Box plots  
64 represent the first quartile, median, and third quartile, with whiskers indicating minimum and maximum  
65 values. Results were analyzed with unpaired *t* test and expressed as  $\pm$  SEM ( *n* = 4 - 5 ).  
66 ns, non significant; \*\*, *p* < 0.01; \*\*\*, *p* < 0.001.

67

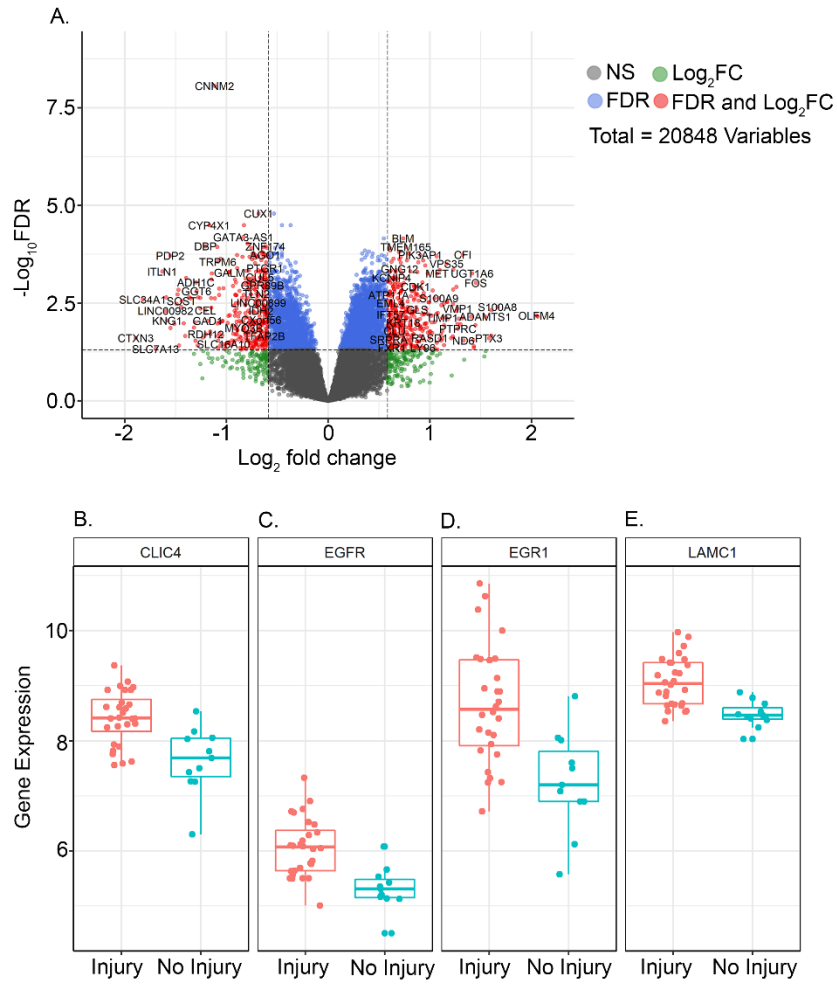


68

69 **Supplemental Figure 3. MiRNA cocktail 1 and cocktail 2 attenuate or mimic the effects of HFpEF<sub>CRS</sub>**  
 70 **EVs: (A) *CST3* expression was significantly decreased in the “HFpEF<sub>CRS</sub>+miRNAs cocktail 1 treated**  
 71 **group” compared to “HFpEF<sub>CRS</sub>+Control cocktail 1 treated group”;** n = 3-4 for each group. **(B) *CST3***  
 72 **expression was markedly increased in the “Healthy Control+MiRNAs cocktail 2 treated group” compared to**  
 “Healthy Control+Control cocktail 2 treated group”.; n = 3 for each group. *GAPDH* was used as internal loading control. Results were analyzed by unpaired *t* test and expressed as ± SEM of three independent experiments. \*\*, p < 0.01.

76

77



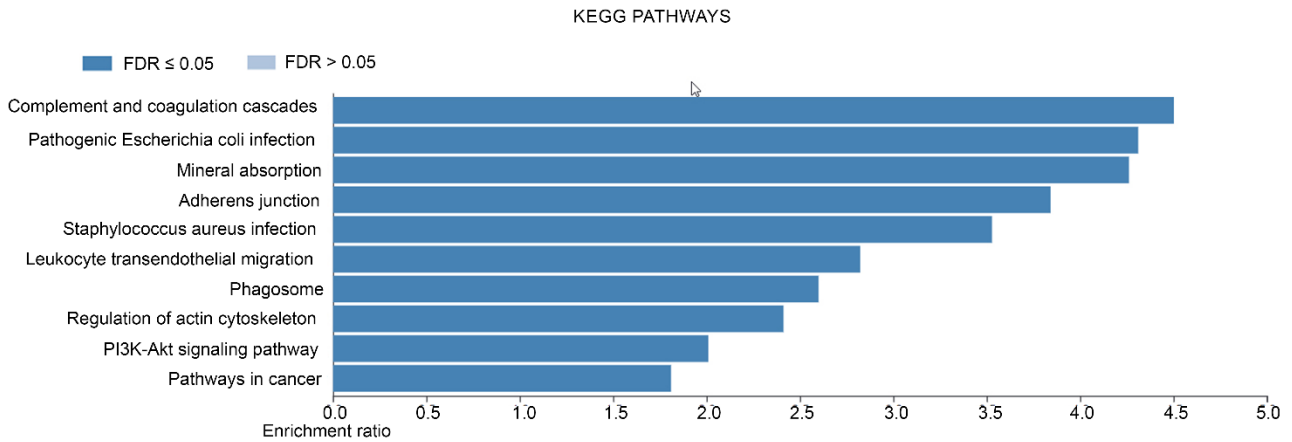
78

79 **Supplemental Figure 4: (A) Volcano plot was created by all differentially expressed genes.** Y axis  
 80 shows Log<sub>10</sub> FDR and X axis displays the log<sub>2</sub>-fold change value. The red dots represent the  
 81 differentially expressed genes with FDR adjusted p value ≤ 0.05 and absolute fold change ≥ 1.5, while green  
 82 dots represent non significantly modulated genes. **(B-E)** Box and whisker plots showing differential  
 83 expression of genes in the “Injury” and “No Injury” groups. Box plots represent the first quartile, median,  
 84 and third quartile, with whiskers indicating minimum and maximum values.

85

86

87



89 **Supplemental Figure 5. Pathway analysis by WebGestalt.** The enrichment bar chart is shown for the top  
 90 10 enriched KEGG pathways with  $FDR \leq 0.05$ . As the enrichment increases, the corresponding function is  
 91 more specific. KEGG, Kyoto Encyclopedia of Genes and Genomes; PI3K, Phosphatidylinositol 3-kinase;  
 92 AKT, protein kinase.

93

94

95

96

97

98

99

100

101

102

103

110 **Supplemental methods**

111 **RNase A Treatment**

112 Isolated EVs (210  $\mu$ L) were incubated with RNase A at a 0.5 $\mu$ g/ $\mu$ L final concentration to degrade any  
113 extracellular RNAs not protected within EVs (Thermo Fischer Scientific, Waltham, MA, USA) for 20  
114 minutes at 37 °C followed by an addition of RNase inhibitor (Thermo Fischer Scientific) at a 20U/ $\mu$ L  
115 concentration to inactivate RNase A prior to RNA extraction.

116 **Microfluidic resistive pulse sensing (MRPS)**

117 EVs were diluted at 1:100 to prevent saturation of the upper limit of detection or aggregation, subjected to  
118 MRPS using the Spectradyne's nCS1 (Spectradyne, Signal Hill, CA, USA), and analyzed with both high  
119 and low sensitivity settings (NP100; voltage, 0.60 V; stretch, 46.0 mm and NP400; voltage, 0.40 V; stretch,  
120 43.5 mm respectively). The pressure was preset at 7.0 mbar. Minimum 2000 particles were analyzed for  
121 each sample.

122 **Transmission electron microscopy (TEM) of plasma EVs**

123 A drop containing 5  $\mu$ L of purified plasma EVs (for both c-DGUC and SEC) was placed on parafilm, and  
124 a carbon-coated copper grid was placed on top of the drop for 30 minutes. Carbon-coated copper grids were  
125 previously glow discharged for 30 seconds to turn into an overall hydrophilic surface. For immune gold  
126 labeling, grids were blocked with 1% BSA in 1X PBS for 10 minutes, and IgG primary antibody anti-CD81  
127 (Santa Cruz Biotechnology, Dallas, TX, USA; 1:30 dilution in blocking reagent) was used for 30 minutes  
128 at room temperature. Grids were then washed three times in 1X PBS and incubated with Protein A,  
129 conjugated with 10 nm gold particle (1:30 dilution) for 20 minutes at room temperature. Grids were washed  
130 twice with 1XPBS (for 5 minutes total) and 4 times with water (for 10 minutes total). Grids were stained  
131 with 0.75% uranyl formate for 1 minute and visualized on a JEOL 1400 electron microscope outfitted with  
132 an Orius SC1000 CCD camera (Gatan, Inc. Pleasanton, CA, USA).

133

134

135

136 **Immunofluorescence analysis**

137 Epithelial cells, grown on coverslips were treated with EVs from either Healthy Control or HFpEF<sub>CRS</sub>  
138 patients and then stained with the primary antibodies (NGAL, IL-18 and KIM-1) followed by incubation  
139 with Alexa Fluor 555-labeled secondary antibodies (Molecular Probes) (Supplemental Table 5). After the  
140 slides were mounted with Vectashield (with DAPI [4',6-diamidino-2-phenylindole]) (Vector Laboratories,  
141 Newark, CA), the slides were examined under a fluorescence microscope (BioRad).

142 **Long RNA sequencing of plasma EV samples**

143 Long RNA sequencing on the exRNAs isolated from the plasma of HFpEF patients with high creatinine (n  
144 = 9, 1.1-1.6 mg/dL) and low creatinine (n=9, 0.7-0.9 mg/dL) were performed using the miRNeasy  
145 Serum/Plasma kit (Qiagen). cDNA libraries were constructed using the SMARTerStranded Total RNA-  
146 Seq Kit v2 Pico Input Mammalian (Takara Bio, San Jose, CA, USA) and sequenced using NextSeq 2000  
147 platform.

148 **Deconvolution analysis for the identification of source organs:**

149 A similar approach to identify the source tissue has been previously (1) performed to generate the log  
150 transformed gene expression values for each sample in the Creatinine high and low groups, the DESeq2  
151 (<https://genomebiology.biomedcentral.com/articles/10.1186/s13059-014-0550-8>) rlog function was used.  
152 Tissue-specific genes were obtained from the protein atlas  
153 website(<https://pubmed.ncbi.nlm.nih.gov/25613900/>), and a random sample of up to 172 tissue-specific  
154 genes (corresponding to the bottom 25% percentile of the number of tissue-specific genes across tissues)  
155 was selected for each tissue. The tissue enrichment score for each sample was calculated using the log  
156 transformed gene expression values and tissue specific genes, following the algorithm of PangoDB  
157 (<https://academic.oup.com/database/article/doi/10.1093/database/baz046/5427041?login=false>). This  
158 process of tissue specific gene sampling and tissue enrichment score calculation was repeated 1000 times.  
159 The median tissue enrichment score for each tissue and sample was then calculated from these 1000 repeats.

160 Finally, the tissues were ranked based on the median of median tissue enrichment scores of samples in the  
161 creatinine high group, and these rankings were visualized using a violin plot.

162 The tissue-enriched genes of adipose tissue, heart muscle, kidney, liver, pancreas and skeletal muscle were  
163 downloaded from The Human Protein Atlas (<https://www.proteinatlas.org/>) (2). For each tissue, the tissue-  
164 enriched genes were ranked by the RNA tissue specificity score and the top 5 genes were selected to  
165 represent the tissue. The TPM values of these genes for each sample in the Creatinine high and low groups  
166 were calculated using the convert Counts function from the DGEobj.utils package and visualized by ggplot2.

### 167 **Cellular transfection of miRNAs inhibitors and mimics:**

168 To confirm the role of miR-192-5p, 21-5p and 146a-5p in regulating the expression of kidney injury  
169 markers and TGF beta pathway related proteins, epithelial cells were treated with corresponding miRNA  
170 inhibitors and miRNA mimics in the various conditions. Epithelial cells transfected with a mixture  
171 (MiRNAs cocktail 1; Qiagen, Hilden, Germany) of synthetic miRNA inhibitors (single strand  
172 oligonucleotides) formiR-192-5p (5'-GGCTGTCAATTCATAGGTC-3'), miR-21-5p (5'-  
173 ACATCAGTCTGATAAGCT-3') and miRNA mimic for miR-146a-5p (5'-  
174 UGAGAACUGAAUCCAUGGGUU-3') followed by treating with HFpEF<sub>CRS</sub> derived EVs. Both  
175 Healthy Control and another group of HFpEF<sub>CRS</sub> derived EVs treated cells were pretreated with a mix  
176 (Control cocktail 1) of LNA miRNA Inhibitor Controls (Qiagen) and scrambled NC siRNA (All Stars  
177 Negative Control siRNA, Qiagen) (Figure 10A).

178 On the other hand, one group of epithelial cells pretreated with a mixture (MiRNAs cocktail 2) of synthetic  
179 miRNA mimics for miR-192-5p (5'-CUGACCUACGAAUUGACAGCC-3'), miR-21-5p (5'-  
180 UAGCUUAUCAGACUGAUGUUGA-3') and inhibitor for miR-146-5p (5'-  
181 ACCCATGGAATTCAGTTCTC-3') followed by treatment with Healthy Control derived EVs and other  
182 group, pretreated with Control cocktail 2 (LNA miRNA Inhibitor Control and scrambled NC siRNAs,  
183 Qiagen) further treated with Healthy Control derived EVs (Figure 11A). Cells were maintained for 72 hours.  
184 All transfections were performed using Lipofectamin RNAiMax transfection Reagent (Invitrogen,  
185 Waltham, MA, USA) following manufacturer instructions.

186

187 **References cited for supplemental methods:**

188 1. Gokulnath P, Spanos M, Lehmann HI, Sheng Q, Rodosthenous R, Chaffin M, et al. Plasma extracellular  
189 vesicle transcriptome as a dynamic liquid biopsy in acute heart failure. *medRxiv*. 2023.

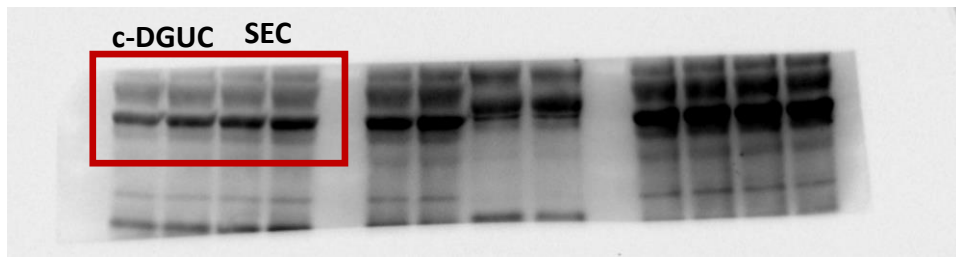
190 2. Uhlén M, Fagerberg L, Hallström BM, Lindskog C, Oksvold P, Mardinoglu A, et al. Proteomics. Tissue-  
191 based map of the human proteome. *Science*. 2015;347(6220):1260419.

192

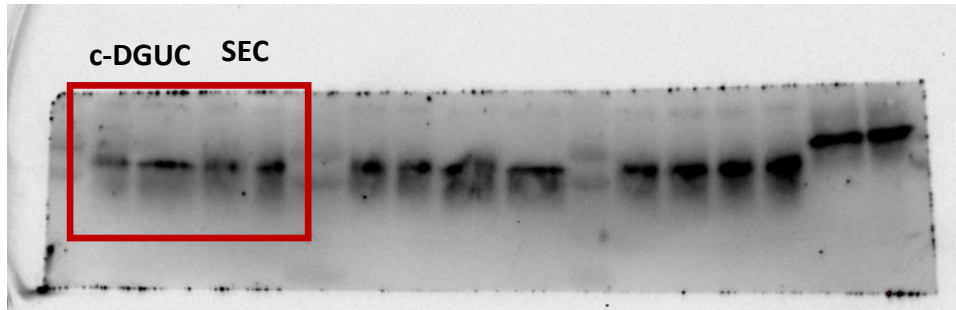
193

194

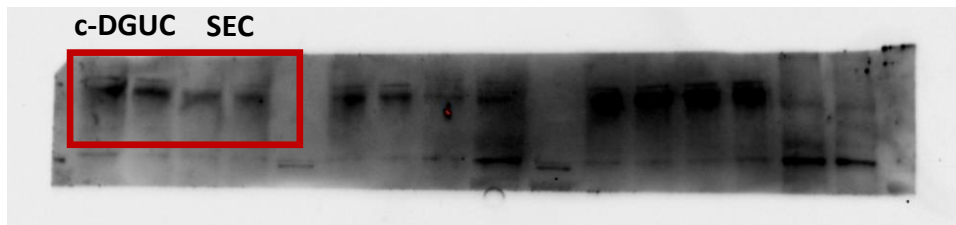
195



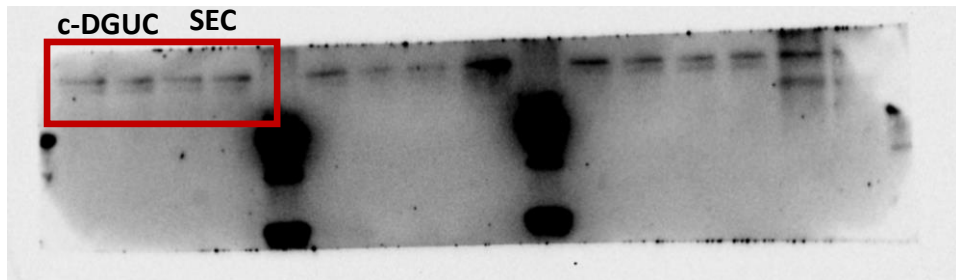
CD63



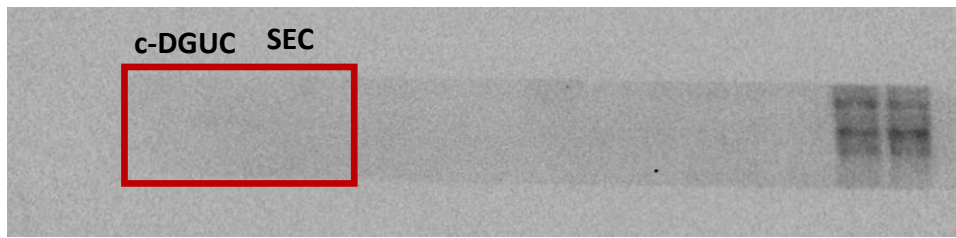
CD81



Alix



Syntenin



58K Golgi Protein